Royal Netherlands
Meteorological Institute
Ministry of Infrastructure and the Environment

Monitoring induced seismicity in the North of the Netherlands: status report 2010

Bernard Dost, Femke Goutbeek, Torild van Eck and Dirk Kraaijpoel

De Bilt, 2012 | Scientific report; WR 2012-03

Monitoring induced seismicity in the North of the Netherlands: status report 2010

Version 1.0

Date July 2012
Status Final

Summary

This report presents an update on the results from monitoring induced seismicity in the North of the Netherlands. The latest report on this issue (Van Eck et al., 2006) is based on seismicity data from 1986 to 2003. In the mean time, the dataset more than doubled. The analysis is extended to include data up to 2010 and it has been decided to update reports every 5 years. The borehole monitoring network has been expanded, now also covering the northern part of the province of Friesland, and upgraded to a full real-time system. Expansion includes borehole seismograph stations and accelerometer stations. The upgrade enables a faster response at felt earthquakes and the determination of automatic first locations, which is subject of further development. New detection and location threshold maps have been calculated.

Seismicity continued to develop and shows a clear connection with existing faults at reservoir level. Since 2003 the Groningen field dominates in activity, with an increase in mainly smaller magnitude (M <1.5) events. This behaviour is reflected in the calculation of the Gutenberg-Richter parameter b, which shows a significant difference between the Groningen field (b=1.0) and the other fields (b=0.6). Other parameters of importance to hazard calculations did not change significantly. The maximum magnitude M_{max} is stable at a value of 3.9. New attenuation relations for small shallow events are being constructed within the EC funded GEISER project. New hazard maps will be constructed when these relations are available. The hazard analysis assumes that the seismicity rate is a stationary process. We do see, however, from the cumulative seismic energy a change in character over time and it its effect will be taken into account in future studies.

The source mechanism of induced earthquakes provides important information on the reactivation of existing faults and constraints for geomechanical modelling of reservoirs. An overview of results for different gas fields in the Netherlands is given, including new results for the largest earthquakes in the Groningen field. The influence of a thick salt layer, acting as a high velocity layer on top of this reservoir, complicates the analysis and a special modelling study was needed to correct for this effect. Waveform modelling of the accelerometer recordings in the region is expected to improve depth estimates of the induced events.

This report concludes with a discussion of the present results and gives recommendations for improved monitoring and further research. The focus in monitoring is on expanding the real-time data exchange to include the accelerometer network and on microseismic monitoring, while for further research a continuation of the hazard research and waveform modelling is proposed.

Contents

1. Introduction

Induced seismicity in the north of the Netherlands started in 1986. Its origin is related to gas exploitation from a number of on-shore gas fields, including the Groningen field, which is the largest on-shore gas field in Europe. Although most of the earthquakes are shallow and small, the larger earthquakes (M_L > 2.5) occasionally cause damage. This is of concern to the population, the Dutch government and the mining companies. The new mining legislation (Staatsblad 542[1], 2002) requires a hazard/risk analysis for each new exploitation license and a measurement plan to detect earth movements. The KNMI is responsible for the monitoring of seismicity for the Netherlands, operates different seismic networks and carries out hazard studies.

In previous reports and publications (De Crook et al., 1998; Van Eck et al., 2004, 2006; Dost and Haak, 2007) the characteristics of the induced seismicity have been discussed. The latest hazard study was based on the seismicity from 1986-2003. Since that time, the total number of events nearly doubled (from 330 to 640, status 1.1.2010) and the need for an update of the analysis was strongly felt. We focus on the northeast of the Netherlands, since there has not been any new seismicity recorded in the north-west since 2001. Since 2010 the KNMI is involved in the monitoring of microseismicity at the Bergermeer gas-storage facility. Results will be discussed in the next hazard update.

During the last 10 years requests for information on induced seismicity, its hazard and potential impact has been successively increasing. From an initial simple monitoring of larger felt events, we are currently being asked to provide detailed information on seismicity, quantifying hazard and give relevant input to exploration regulations. All within a tight cost-benefit framework. Consequently, we have been considerably improving our monitoring network to suit these requirements and started a whole range of new studies to answer the questions asked by the society. These initiatives are described in this report.

[1] http://www.eerstekamer.nl/wetsvoorstel/26219_mijnbouwwet

2. Network developments

Since 1995 a monitoring network of 8 borehole stations is in operation in the north-eastern part of the Netherlands. Each borehole station is equipped with four levels of 3C sensors (4.5 Hz SM6 geophones, see Dost and Haak, 2002). The separation between the different levels is 50 m for 7 boreholes (50-100-150-200m depth), while the first borehole that came in operation (FSW, Finsterwolde) has a separation of 75 m between the levels and a maximum depth of 300m. The boreholes have no casing.

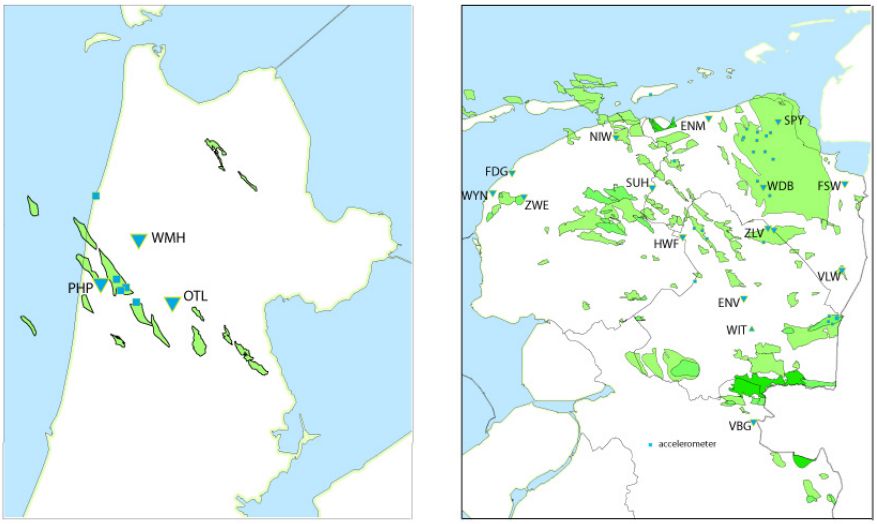

Figure 1. KNMI monitoring network. Triangles show borehole installations, squares accelerometer stations. Gas fields are shown in green. New borehole stations are FDG,WYN,ZWE,NIW,SUH and SPY.

In 2010 a major upgrade has been implemented that consist of an extension of the network with 6 stations, real-time continuous data transmission from sensor to the data centre, the implementation of an automatic detection and location tool, and the extension of the accelerometer network since 2006. The network in the northern part of the Netherlands as depicted in Figure 1 consists currently of 17 borehole stations and 23 accelerometers.

Seismograph network extension
The network was extended in 2010 with six borehole stations: one in the north-western part of Groningen (SUH, Surhuizum); one in the north-eastern part of Groningen (SPY, Spijk); one in the north-eastern part of Friesland (NIW, Niawier) and three near Harlingen (west Friesland; Wijnaldum (WYN), Firdgum (FDG) and Zweins (ZWE)). All these new boreholes are 120 m deep and are equipped with four levels of 3C sensors at 30 m spacing. A cost-benefit analysis motivated the shallower depth boreholes, i.e. 120 m instead of 200 m. A borehole of limited depth (max 120 m) is significant cheaper to realise than 200 m, while the signal to noise ratio hardly increases. The three stations near Harlingen are installed on request of the ministry of Economic Affairs in order to monitor local seismicity due to salt mining. The other additional stations were installed to improve the detection and monitoring capacity of the north of the Netherlands.

Real-time continuous data transmission
The upgrade of the existing borehole network consists of connecting the electronics to a Digital Subscriber Line (DSL) and creating a real-time data transmission to the central site in de Bilt. Data transmission has been arranged through the seedlink protocol, enabling a smooth streaming of the data into existing analysis packages (e.g. Seismic Handler[2] and SeisComp3[3]).

Automated detection and location
Since 2009 we are upgrading the old system, which was based on single station event triggering and manual digital data retrieval by telephone, with the above described continuous data transfer and automatic multi-station detection and preliminary location using the SeisComp3 software. The SeisComp3 software was originally developed by the GeoForschungs Zentrum (GFZ) in Potsdam for automatic detection and location of large tsunamigenic earthquakes near Indonesia (Hanka et al., 2010). Currently we are evaluating and tuning the system to work also on regional, local and induced seismicity.

Accelerometer network
In addition to the seismometer network, designed to locate earthquakes in the region, there is a need to measure the acceleration of the soil in the epicentre area of felt earthquakes. This information is essential for hazard calculations, but also serves as input for modelling the impact of these earthquakes on structures (e.g. Van Staalduinen and Geurts, 1998; Roos et al., 2009). Also, accelerometer recordings can be used to study waveform propagation at close epicentre distances. Figure 1 shows the status of the seismometer and accelerometer network (1.1.2010).

In the period 2004-2010 a total of eight new accelerometers have been installed in the province of Groningen. One additional accelerometer was installed at Schiermonnikoog, northwest of Groningen and part of the province of Friesland. In 2011 one more accelerometer was installed at the island.

[2] http://www.seismic-handler.org
[3] http://www.seiscomp3.org

3. Detection and location thresholds

In Van Eck et al. (2004), appendix 3, the detection and location capacity of the network is evaluated, using a simple model based on estimating the average noise level at the lowest level (200m) of the boreholes combined with a regional attenuation relation. The upgraded network, including the upgrades in the southern part of The Netherlands not described here, require a re-evaluation of the detection and location capacity of the network.

Reports on felt events from the general public in the north of the Netherlands show felt events starting from a magnitude of 1.8 on the Richter scale (M_L). Although this magnitude is very low for natural events, the limited depth of the induced events (2-3 km) is causing this phenomenon. As a result the network should at least be capable of recording events of magnitude a little below the threshold for felt events. Therefore, the network design is based on a detection and location threshold of M_L=1.5 for the region of interest.

These detection and location thresholds estimates are based on the measured average noise levels in the boreholes and a number of assumptions, as explained in van Eck et al., 2004. In summary:

1. Background noise varies in time, so average values are used.
2. Assuming a signal to noise ratio of 2, the average noise level in the boreholes is estimated at Amp_{wa} =0.02mm at 120 and 200m depth, while for surface stations an average noise level of Amp_{wa} =0.1mm has been estimated. Amp_{wa} indicates the amplitude of a simulated wood-anderson seismograph.
3. Noisy surface sites (DBN,WIT, 0171 (Nieuwstad) and RDC) are characterized by a 3* higher noise level.
4. Stations operated by partners outside the Netherlands (ROB, Brussels and Bensberg, Uni Köln) have not been included.
5. Detection threshold implies that at least one station recorded the event, while for the location threshold a minimum of 3 stations should have recorded the event.
6. For the borehole instruments the following attenuation function has been used (Dost et al., 2004): $M_L = \log(Amp_{wa}) + 1.33\log(\Delta) + 0.00139\Delta + 0.924$
7. For surface stations: $M_L = \log(Amp_{wa}) + 1.5\Delta$

Results are shown in figure 2. Detection capacity for the active part of the north of the Netherlands is now at the M_L=1.0 level, including the north and north eastern part of the province of Friesland. A similar improvement is visible for the location capacity.

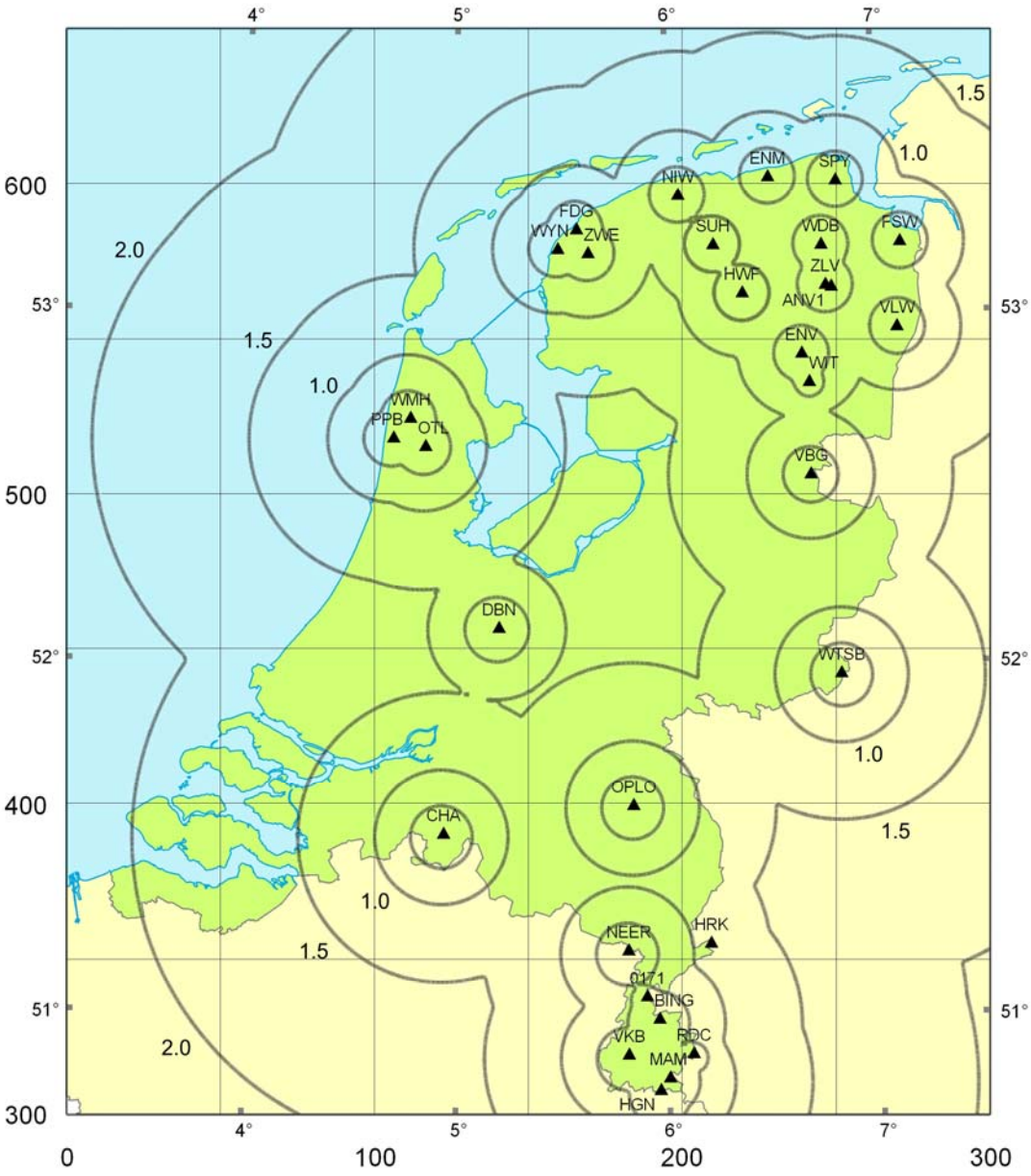

Figure 2a. Detection threshold for the current network. Station 0171 is situated in Nieuwstad (Limburg).

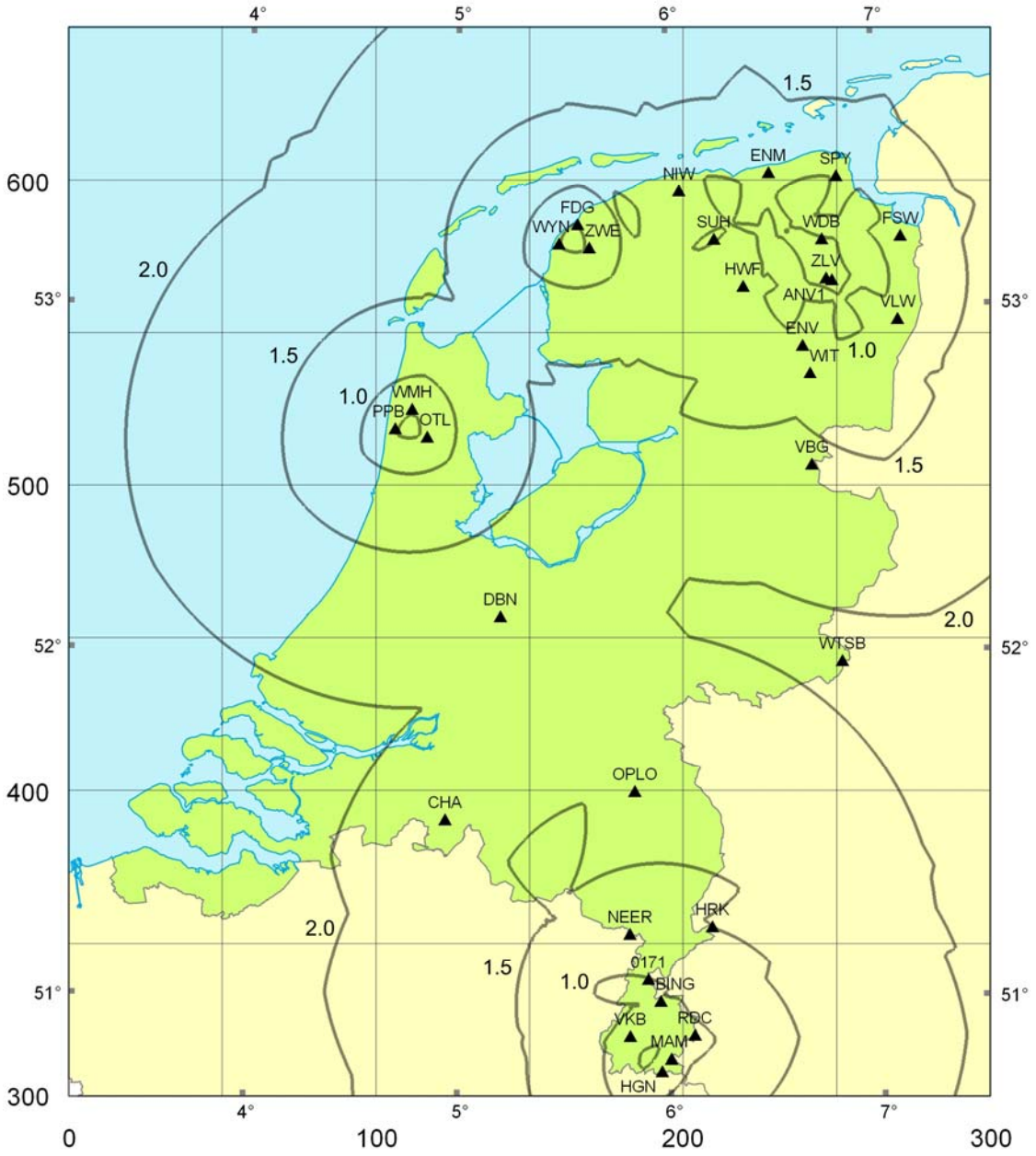

Figure 2b. Location threshold. Station 0171 is situated in Nieuwstad (Limburg).

4. Updating the seismicity characteristics for 1986-2009

Since the last seismicity overview for the years 1986 – 2003 the total number of recorded and identified events in the north of the Netherlands has nearly doubled, from 330 to 640 events. It is therefore opportune to re-assess the characteristics of the induced seismicity, including an evaluation of input parameters for hazard analysis, like the maximum magnitude (M_{max}) and the coefficients of the cumulative frequency-magnitude relation. Specifically, the additional data provides an excellent opportunity to verify, refute or renew the models we proposed earlier.

4.1 Seismicity patterns

An important clue to the cause and process of induced seismicity is its relation to the existing tectonics and exploration. This motivates our continuous quest to identify seismicity patterns in space and time. In general the seismicity in the north of the Netherlands continues to show similar patterns with respect to the previous report (Van Eck et al., 2004). Nearly all events are located in or around existing gas fields in production (figure 3). However, a few exceptions can be identified, e.g. in the Lauwerszee-trough, west of the Groningen Field (see Dost and Haak, 2007). Their origin is unclear, but may be connected to changes in the aquifer around the Groningen field.

It becomes clear that most events occur near existing faults in the top of the reservoirs at base Zechstein, which is indicative for the reactivation of existing faults. In the Groningen field the south-eastern part of the field does not show any activity, while existing faults are available for reactivation. This observation has led us to extend the monitoring network to the northeast, as described above, in order to be able to verify that this is real and not due to deficiencies in the monitoring network.

A remarkable observation is the occurrence of a series of small events in 2009 near Midlaren, see Appendix A. A swarm of 41 events occurred near Midlaren over a period of one month (22 February – 22 March), with a peak activity of 17 events on March 17. This swarm is most probably related to an experiment, carried out by NAM, approximately 5 km from the epicentre locations. The maximum magnitude of the events in this swarm was 1.4, below the completeness threshold. Consequently, the swarm may contain many more lower magnitude events not detected by the network. Due to its specific nature, these data are not used in the following seismic hazard analysis.

An event in the southern part of Friesland, close to the towns "de Hoeve" and "Weststellingwerf", see Appendix B, is possibly connected to water injection instead of gas production.

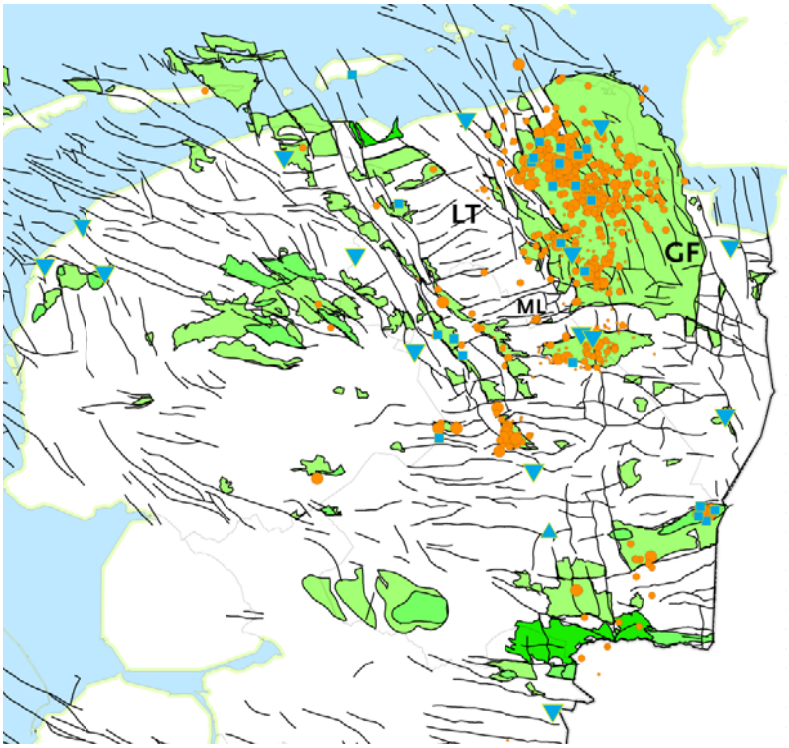

Figure 3. *Epicentre map of induced earthquakes in the north-eastern provinces of the Netherlands. Gas fields are shown in green. Faults shown are at base Zechstein (thin black lines), corresponding to the average hypocentre depth of ca. 3 km. Blue triangles indicate seismic stations and blue squares accelerometer stations. Indicated are the Groningen field (GF), Lauwerszee trough (LT) and Midlaren (ML).*

4.2 Seismicity variation with time

A thorough analysis of the seismicity variation in time is necessary to evaluate possible patterns related to exploration. However, a crucial factor in this is played by the observational and detection capacity of the implemented monitoring network. An estimate of the degree of incompleteness is therefore important and our main concern in this chapter.

The development in time of the overall seismicity can be shown in different ways. Figure 4a shows the magnitude of the events as a function of time. In addition the completeness of the dataset is indicated. This changes over time and is influenced by the development of the network. In 1995 the current borehole network was constructed, realizing a M_L=1.5 detection threshold for the region of interest: the provinces of Groningen and Drenthe. Recent expansion of the network enlarged the region covered, but did not lower the detection and location threshold due to the large distance between seismic stations (app. 20 km).

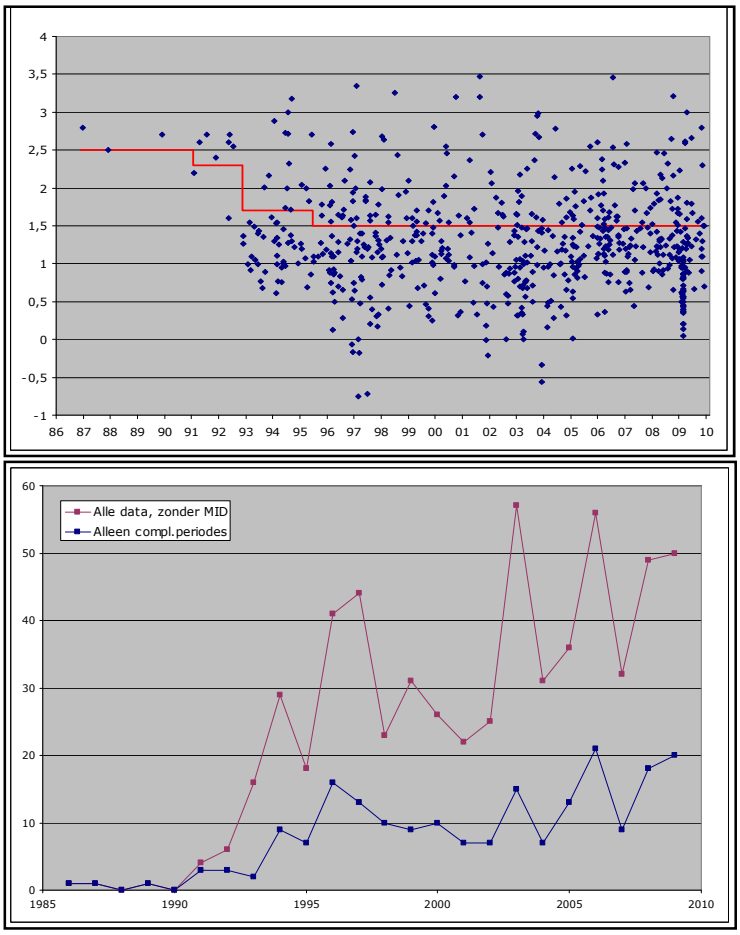

Figure 4. Seismicity in the northern part of the Netherlands. a](top) Displayed in time as a function of magnitude. The red line gives the completeness of the network in time. b](bottom) Number of earthquakes as a function of time. In red all events without the Midlaren swarm are displayed, in blue only events with magnitudes above the completeness threshold.

Nearly 67% of the located events has magnitudes below the detection threshold. This means that we record lower magnitude seismicity close to the boreholes, but not all small events that may happen in the region of interest. Annual variations in the number of induced events, figure 4b, show a large variation and even an increase over time. Limiting the events to only those with magnitudes above the completeness threshold significantly reduces this variation. Therefore, we conclude that most of this variation is due to small events. It was decided to leave out the data from the Midlaren swarm, since these are thought to be related to a specific experiment.

Since 2003 the majority of the seismic events seems to be concentrated in the Groningen field (GF). The number of events and their strengths (magnitudes) in this field increased. At the end of 2009 a total of 341 of the total of 640 events could be connected to the GF. This allows a detailed comparison between the behaviour of this largest field in the Netherlands and the total region. Figure 5 shows the contribution of GF events to the total dataset. It corroborates the feeling that since 2003 seismicity is dominated by this field.

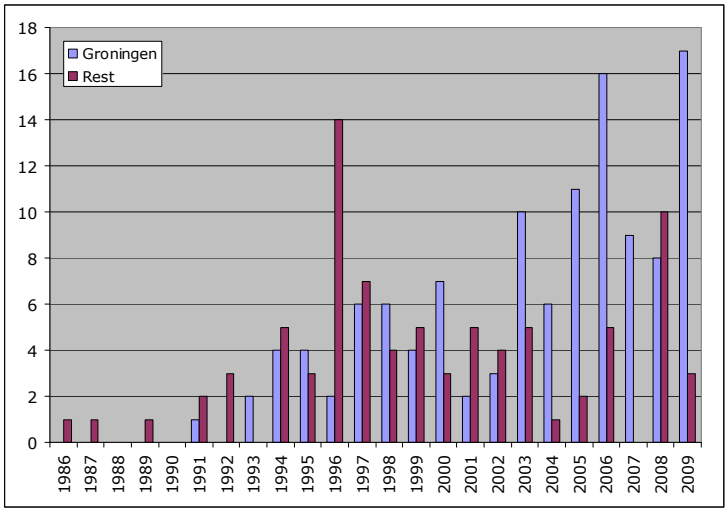

Figure 5. Total number of earthquakes per year. A distinction is made between activity associated with the Groningen Field and activity related to all other fields, i.e. the rest. Only events that are above the completeness threshold are counted.

The previous analysis describes some general features of seismicity. In order to retrieve parameters that are of interest in hazard studies, like M_{max} and the coefficients of the frequency-magnitude relation, we carried out the following analysis.

4.3 Frequency-magnitude relation

Seismic hazard analysis requires a model that includes an estimate of the frequency-magnitude relation in the region. In Van Eck et al (2004; 2006) we did not find strong arguments for using a more complex model than the relatively simple lognormal cumulative annual frequency-magnitude relation given the limited set of events. We pursued this assumption also here. As in the previous studies this relation shows a linear behaviour for $1.5<M_L<2.7$: $log(N) = a - b*M_L$. For $M_L>2.7$ there is no more linearity and the curve drops steeply. The relation can be modelled as a double truncated lognormal function (e.g. Consentino et al., 1977).

In earlier studies (De Crook et al, 1998) the *a* and *b* values were determined by least squares techniques from the linear part of the curve. However, better estimates of parameter *b* can be obtained using maximum likelihood estimators (e.g. Marzocchi and Sandri, 2003) taking into account the full curve. This implies knowledge on the minimum magnitude M_{min} and the M_{max}. Most of these methods are based on an approximation where M_{max}-$M_{min} \geq 3$, which does allow to relax the a-priori knowledge on M_{max}. Unfortunately, this is not valid in our case. Page (1968) on the other hand does not use this approximation and *b* is estimated by:

$$b = {}^{10}\log e\{\overline{m} - \frac{m_{\min} - m_{\max} e^{-b'(m_{\max}-m_{\min})}}{1-e^{-b'(m_{\max}-m_{\min})}}\}^{-1}$$, where $\overline{m}$ is the average magnitude and

$$b' = b/{}^{10}\log e$$

The effects of a finite magnitude range and sampling of a continuous function was discussed at length (e.g. Bender, 1983) and corrections are proposed. In our case the magnitude sampling of 0.1 unit is small enough to have no significant effect. Results from the analysis of the *b* are shown in table 1, where three often used methods are compared.

	All fields	Groningen field	Other fields
Page (1968)	b = 0.77 ± 0.08	b = 1.02 ± 0.16	b = 0.52 ± 0.07
Marzocchi et al. (2003)	b = 0.77 ± 0.05	b = 0.94 ± 0.08	b = 0.61 ± 0.07
Weichert (1980)	b = 0.84 ± 0.06	b = 1.05 ± 0.09	b = 0.63 ± 0.08

Table 1. Overview of the b-parameter in the Gutenberg-Richter relation for induced events in the Netherlands.

For all fields the total number of events with M>1.5 is 214 and there is little difference between the solutions within the error bounds. For the Groningen field the total number of events is reduced to 131, leaving 83 events for the other fields. The method of Page (1968) is dependent on the choice of M_{max}. In this analysis a value of M_{max}=3.7 was used, being the mean of the distribution for the dataset 1986-1997 (Van Eck et al., 2004). Evaluation of the procedure using M_{max}=3.9 gives as results for all fields b=0.79 ± 0.09, for the Groningen field b=1.03 ± 0.16 and for the other fields b=0.56 ± 0.09.

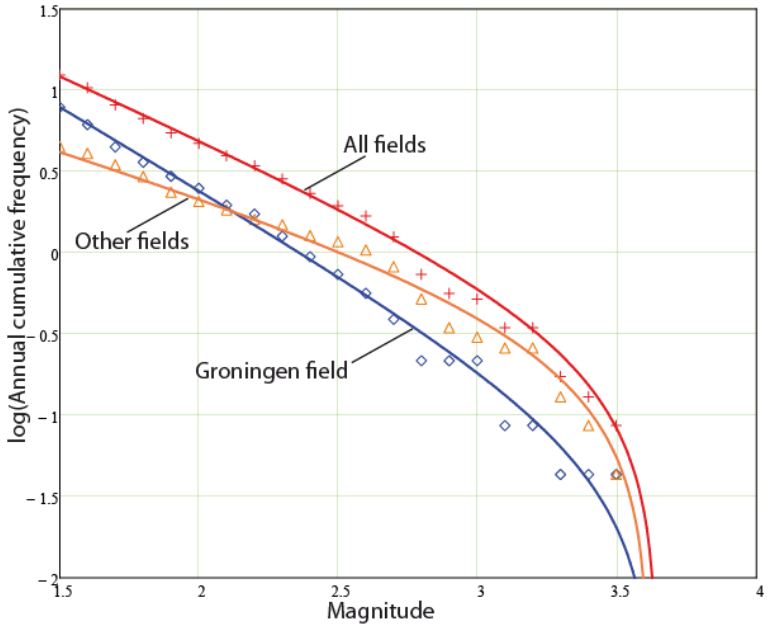

Figure 6. Annual cumulative frequency as a function of magnitude for all fields together (red), only the Groningen field (blue) and the remaining other fields (orange).

Estimates of parameter a are less common. Weichert (1980) notes that "its maximum likelihood estimate is simply the total number of events observed above the threshold of completeness". Taking the b-value estimates using the method of Page (1968) at M_{max}=3.7, leads to the following estimates: for 'all fields': a=2.25 ± 0.12, for the Groningen field: a=2.43 ± 0.14 and for the remaining other fields: a=1.43 ± 0.12. Compared to the earlier studies for 'all fields' both the a- (2.16 ± 0.15) and b- (0.80 ± 0.08) value did not change significantly. For the Groningen field these values were a=2.16 and b=0.98, if we take into account the period 1986-November 2003. The b-value is close to the present value, the a-value significantly lower, although there was no error estimate given (Van Eck et al, 2004, p33).

Although the estimate of the other fields are based on a small dataset, only 82 events, there is a clear distinction between the Groningen field (GF) and other smaller fields. The GF shows a steeper frequency-magnitude curve compared to all the fields, i.e. more small events compared to the larger ones. Smaller fields, like Roswinkel, are characterized by a lack of small events compared to the larger events.

The difference in *b*-values is of importance as input to the hazard calculation. In addition Schorlemmer et al. (2005) find that the *b*-value systematically varies for different styles of faulting. Future research on the variation of the *b*-value with time and location may provide additional information on the state of stress of the reservoirs.

4.4 Maximum magnitude

An extended dataset is an excellent opportunity to test the validity of the maximum possible magnitude earthquake that can be expected to occur as induced event. We follow the methodology that was explained in Van Eck et al. (2004) to estimate M_{max}. Three methods have been used, two statistical methods and one based on a physical model. Only the results from the analysis based on the two statistical methods are updated, since there is no new information available to update the physical model for the North of the Netherlands. However, Muntendam et al. (2008) apply the physical model to assess the hazard for the Bergermeer gasfield and therefore we will give a status update on the use of this method.

Below we study successively the physical and statistical models, and the cumulative seismic energy release concept.

4.4.1 Physical model

The maximum size of an earthquake is determined by the available fault surface, the shear modulus and the average slip. Using $M_0 = \mu A d$ and the relation between M_L and M_0 following Hanks and Kanamori (1979): $M_L = M_w = \frac{\log(M_0) - 9{,}1}{1{,}5}$, the value for M_{max} can be calculated, where M_L is the local magnitude, M_w moment magnitude, μ the shear modulus, *A* the fault surface and *d* the average slip. De Crook et al. (1995) estimated M_{max} for Groningen and the area around Alkmaar, based on μ = 17 GPa, a length scale of the existing faults of 0.8 km and 1.0 km respectively and the depth of the fault at half the length scale. These calculations resulted in an M_{max}=3.5 for Groningen and 3.6 for Alkmaar. Both magnitude estimates were given an uncertainty of 0.5 units. Logan et al. (1997) calculate for the region around Alkmaar a maximum magnitude of M_{max}=3.8. This difference is mainly caused by an assumed higher slip displacement. Muntendam et al. (2008) re-assessed the maximum magnitude calculation for Bergermeer (Alkmaar region) and included the dip of the fault plane, resulting in a M_{max}=3.9.

In the last few years geomechanical modelling of reservoirs in the Netherlands has been carried out. These models give information on the reactivation potential of the existing faults. However, they do not give new information on available fault surface and therefore are not used to re-evaluate the maximum magnitude.

4.4.2 Statistical model

In order to estimate the maximum magnitude, two methods are applied: 1] based on a determination of the coefficients *a* and *b*, the best fitting model is determined including the M_{max} and M_{min} values and 2] using Monte Carlo techniques, a best estimate and error estimates for *a*, *b* and M_{max} are determined.

The Monte Carlo simulation procedure has been described in De Crook et al. (1998) and Van Eck et al. (2004). A total of 2000 experiments were generated by adding random noise to the cumulative frequency measurements and calculating the best fit to a double truncated exponential function. Results show a Poisson distribution of parameters *a*, *b* and M_{max} and provide an average value of the parameters including an estimate of its variance (see figure 7).

Comparison of the Monte Carlo analysis of the total dataset with the dataset for the GF shows a difference in the *b*-value. For the total dataset *b*=0.80 ±0.06, while for the GF *b*=0.98 ± 0.10 was found, similar to the maximum likelihood estimates. For parameter *a* this difference is less pronounced. The total dataset gives *a*= 2.24 ± 0.11 while for the GF *a* = 2.31 ± 0.16. From Monte Carlo modelling the value for M_{max} is the same for both datasets: M_{max} = 3.7± 0.2. Since we add one standard deviation to the average value, M_{max}= 3.9, which is unchanged since the last update.

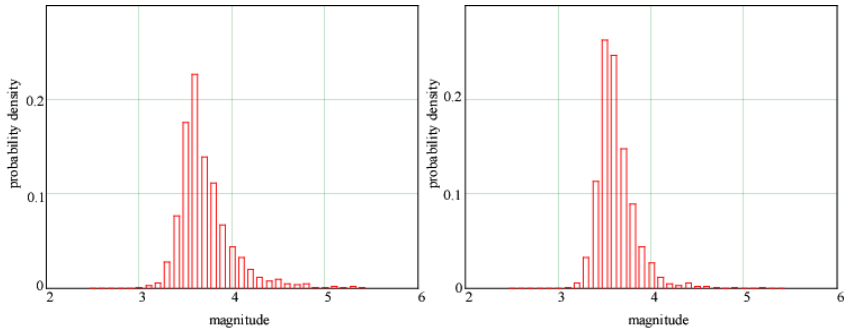

Figure 7. Comparison of the estimation of the maximum possible magnitude for all induced earthquakes in the period 1986-2003, left figure (Van Eck et al., 2004), and the update 1986-2010.

Comparison with the previous study of 2004, based on a smaller dataset (1986-2003), shows a comparable value for M_{max} (3.9) and *b*-value (0.80 ± 0.08) and a somewhat smaller value for the parameter *a* (2.16 ± 0.15). The increased dataset results in a smaller variance (figure 7) and an increase in the number of small earthquakes (parameter *a*).

4.4.3 Cumulative seismic energy release concept

We estimated the cumulative seismic energy release with time for the period 1986-2010 and analysed its implications, following the same procedures as described in Van Eck et al. (2004). Figure 8 shows the estimated seismic energy release, and the upper and lower boundaries to this curve. In a re-interpretation of all data, we find a clear indication of an increased rate of seismic energy release since 2001. The estimated maximum magnitude, however, remains stable at M_{max}=3.8.

The implications of this increased rate of seismicity and thus the breakdown of the stationarity assumption on the seismic hazard estimations should be considered.

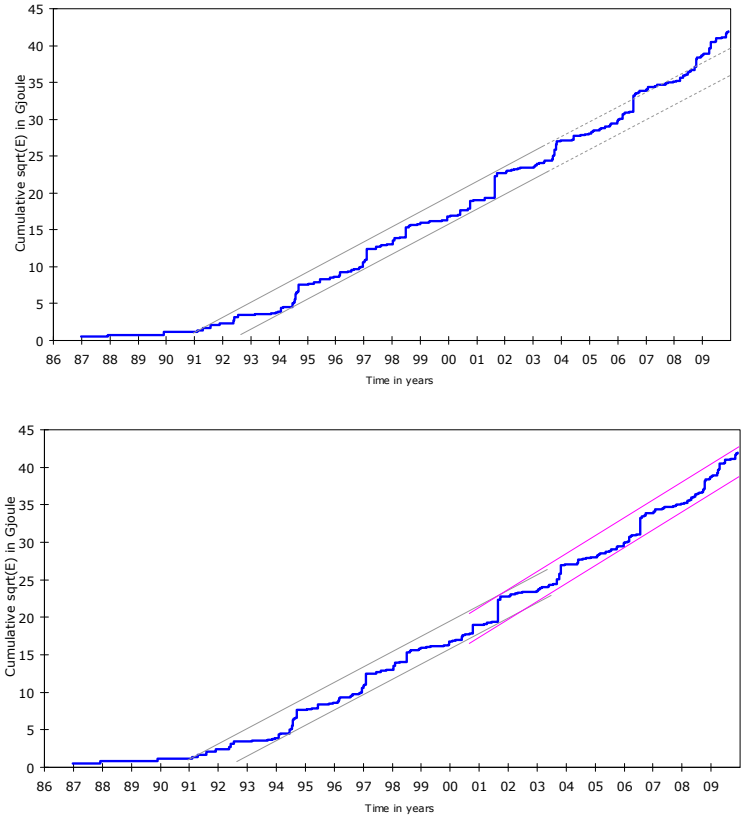

Figure 8. Cumulative square root of the energy released by induced earthquakes as a function of time. All events of M_L>1.5 have been included. The grey straight lines indicate the upper and lower boundaries as determined in Van Eck et al.(2004). Red lines in the right figure show the updated boundary lines valid for the period 2002-2010.

5. Source mechanisms and parameters

The source mechanism of only a few of the larger events has been determined, due to the often limited azimuth coverage. In the BOA report (1993) a first estimate of a mechanism is given for events near the Eleveld gas field. Due to the limited network at the time, only a rough estimate could be given and it was concluded that the most probable mechanism is in line with the known geology. In addition to the mechanism, also parameters as seismic moment, stress drop, radius of a circular fault and the average displacement were calculated, based on the Brune (1970) model.

In this chapter we will give an overview of results for a selected number of fields.

5.1 Alkmaar/Bergen

Four events have been recorded that are related to the Bergermeer gas field, two events in 1994 and two in 2001. The parameters of these events are shown in table 1. Clearly, the stress-drop is low (in the 1-10 bar range), displacement in the 5-10 mm range and the radius of the assumed circular fault is in the range 400-800 m. The mechanism, a reverse re-activation of an existing normal fault, was determined for the 2001 events from polarity data (Haak et al., 2001). Although this mechanism can be explained by differential compaction, it forms a problem in the geomechanical modelling of the reservoir (Muntendam-Bos et al., 2008), where only normal faulting can be modelled in an extensional stress regime.

In a recent review by MIT of the mentioned geomechanical modelling of the Bergermeer field (Hager and Toksöz, 2009), it was recommended to review the mechanism and to carry out a waveform inversion. This study has been carried out by T. Dahm and co-workers at Hamburg university (personal communication, 2011). Results are in agreement concerning the strike and dip of the fault, but do show differences in the movement on the fault plane. Waveform inversion seems to indicate a strike-slip movement with a small vertical component (reverse or normal). It was concluded that further modelling will be required to find a more definite solution. The Bergermeer field is a relatively small gas field and has horizontal dimension of app. 8 km length and 2 km width.

	Magnitude M_L	M_w	Moment [Nm]	Radius [m]	Displacement [mm]	Stress-drop [bar]	Mechanism (strike/dip/rake)
940806	3.0		-	-	-	-	-
940921	3.2		$7.0*10^{13}$	400	8	5	-
010909	3.5	3.5	$1.9*10^{14}$	680	7.4	2.8	130/66/73
010910	3.2	3.1	$6.3*10^{13}$	470	5.0	2 .9	130/66/73

Table 2. Source parameters for earthquakes associated with the Bergermeer field

5.2 Roswinkel

Another small gas field that proved to be active is the Roswinkel field. In the period 1992-2006 a total of 39 events occurred at magnitudes between 0.8 and 3.4. The dimensions of this field are 12 km length and 2.5-3 km in width. The source mechanism is calculated from first motion data, resulting in a reverse mechanism or its equivalent, a shallow thrust mechanism (Dost and Haak, 2007).

5.3 Groningen

Most of the seismic activity in the Groningen field takes place in the north-western part of the field at the northern end of the borehole network. This implies that the azimuth distribution of the borehole records is limited. This situation improves if we combine borehole sensors with accelerometer recordings.

Five events have been selected, based on their strength (M_L > 2,2) and the availability of at least three accelerograms recorded at short distances.

In this analysis an estimate of the takeoff angles is required. At short hypocentral distances (< 8 km), the seismic waves leave the source upwards. Since there is a large salt layer (app. 1 km thick) on top of the gas reservoirs, which acts as a high velocity layer, the waves are reflected away from the normal in stead of becoming steeper in the usual models where velocity increases with depth. Therefore a correction was needed and a realistic 3D model for the Groningen field was modelled using NORSAR 3D software. For both P and S waves the takeoff angle was calculated as a function of distance. After correction for the takeoff angle the source mechanisms calculated are shown in figure 9. Most mechanisms show a normal faulting at a steeply dipping fault with a strike around 290 degrees. Uncertainty is about 20 degrees. The only exception is the 2009-04-14 event, which seems to fit best a normal fault at a strike of 325 degrees.

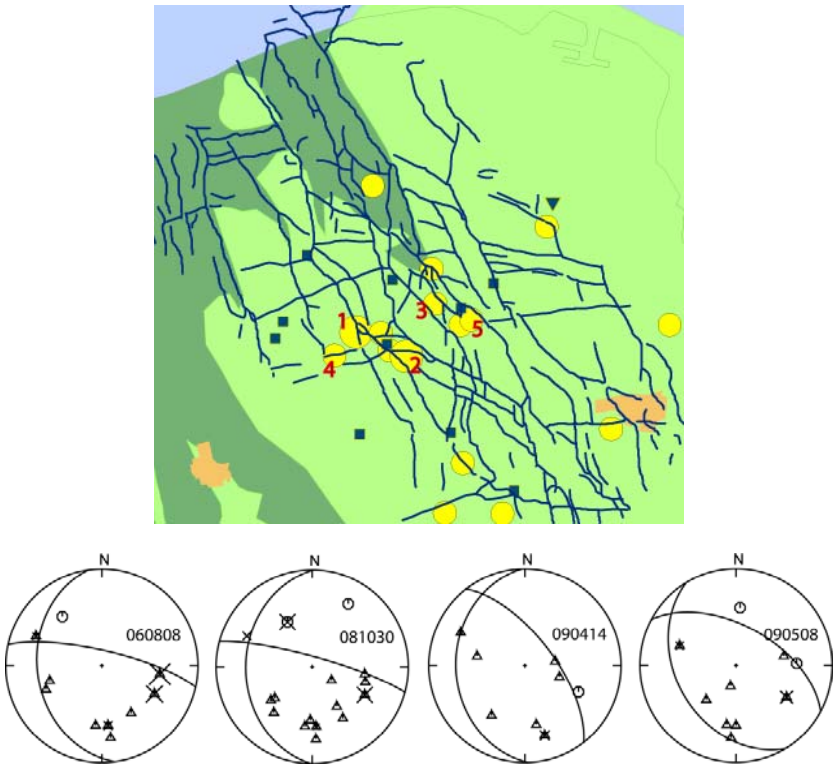

Figure 9. Earthquake mechanisms for 4 earthquakes in the Groningen field and their location. 1=060808, 2=081030, 4=090414, 5= 090508. For event 3 (090201) no stable solution was found. Circles denote positive polarities, triangles negative polarities. Amplitude ratio's are indicated with a cross.

In addition to the mechanism, the spectra of the recordings provide information on other source parameters: seismic moment and derived magnitude, source radius, stress-drop and average displacement at depth. These parameters are measured from spectra that are corrected for the instrument response and absorption/scattering.

The corrections for absorption/scattering are of the form $e^{\pi f R/Q\beta} * e^{\pi \kappa f}$, with R hypocentral distance, Q the quality factor describing regional anelastic attenuation, β the shear wave velocity and kappa (κ) a measure of the decay slope at zero distance (Atkinson, 1996; Anderson and Hough, 1984). The average measured value for kappa for the listed earthquakes in the Groningen field is 0.04s, which does not show a dependency on magnitude or distance and is similar to average values for e.g. California (Atkinson, 1996), Italy (Rovelli et al., 1991) and Mexico (Fernandez et al., 2010).

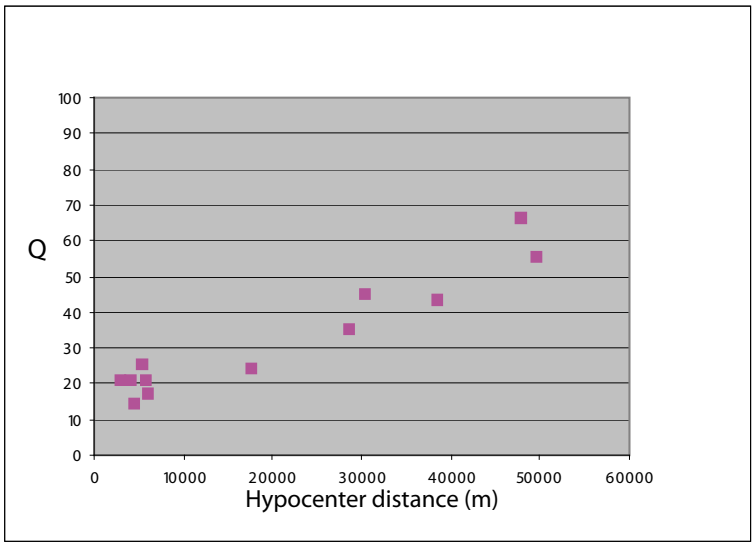

Figure 10. Q measurements for 081030 using the coda Q method

For one event (081030, table 2), Q was calculated for each recording station using a coda Q method (e.g. Van Eck, 1988). At small hypocenter distances (< 25km), Q is approximately constant ~20. With increasing hypocenter distance, Q is slowly increasing (figure 10). However, correction of the spectra with measured Q values does result in a decrease of M_w with distance, which suggests a too large value for Q at larger distances. A constant value of Q=20 for all distances results in a constant magnitude.

Date	Magnitude M_L	Mw	Moment [Nm]	Radius [m]	Displacement [mm]	Stress-drop [bar]	Mechanism (strike/dip/rake)
060808	3.5	3,4±0,2	$1.6*10^{14}$	376±108	32±15	17±12	285/70/-120
081030	3.2	3,1±0,2	$5.5*10^{13}$	327±55	15±6	8±2	285/75/-120
090201	2.2	2,4±0,3	$1.1*10^{13}$	206±29	5±4	4±4	no solution
090414	2.6	2,7±0,2	$2.2*10^{13}$	318±83	5±2	3±1	320/66/-105
090508	3.0	2,9±0,1	$2.7*10^{13}$	330±48	7±2	4±1	295/60/-105

Table 3: Source parameters for earthquakes associated with the Groningen field

Previous measurements of Q in this region were reported by De Crook and Wassing (1996) and Wassing (1998). Values differ from Q=40 measured in borehole FSW between 75 and 300m depth and Q derived from a measured damping ratio of 2-3%, corresponding to Q=17-25, based on recorded artificial signals in the neighbourhood of borehole station ZLV. These values are in accordance with the values measured in the present analysis.

6. Discussion

Since the last report (Van Eck et al., 2004) a number of studies were carried out with respect to induced earthquakes in the Netherlands. Apart from two KNMI studies for specific sites (Van Eck et al., 2007, 2008), a joint TNO-KNMI report (Van Kanten-Roos et al, 2011) was written on the maximum damage that may result from induced earthquakes in the Netherlands with special attention to the Bergermeer gas field, currently in development as a gas storage facility. This 2011 report includes an inventory of recent studies and is added as appendix C to this publication.

Part of the discussion in Van Eck et al. (2004) was focused on "suggestions for further studies". A brief overview will be given on progress:

Continuous monitoring of the seismicity and the ground motion
The monitoring system has been significantly improved enabling effective and efficient near-real time automatic detection and location. Notably the Groningen field is currently more homogeneously monitored through filling obvious monitoring gaps. However, the overall detection level has only marginally improved, as this would require a smaller station spacing not yet accomplished. The installation of a borehole network near Harlingen enables the monitoring of salt mining. A number of initiatives are being launched to take advantage of the improved monitoring system to increase the network density, lowering significantly the detection level and thus enabling closer monitoring of the mechanisms causing seismicity.

The strong ground motion (accelerometer) network has been extended with eight stations which have been optimally installed near locations of concentrated seismicity during the period 2003 - 2010. We have currently a database of 112 acceleration recordings as compared with 43 in 2004. Thanks to its optimal placing the main impact has been a) obtaining focal mechanism solutions, and b) enabling waveform models testing to improve event depth determinations. A thorough re-evaluation of the ground motion prediction equation requires still some more data.

Integration of the near real-time data streams, coming from the borehole network, with a real-time data stream from the accelerometers will be a very useful development in the future. This will enable a faster and more accurate response for the analysis of larger events in the region.

Earthquake mechanism studies
Primarily the availability of more accelerometer recordings of events enabled us to provide more and improved earthquake mechanism estimations. This work will continue.

A combination of improved event detection, providing a basis for a more extensive statistical approach (Schorlemmer et al, 2005; Grob and van der Baan, 2011), and individual earthquake mechanism solutions may seem one promising approach to better understand the reservoir geomechanics.

Attenuation and site response.
Site response was investigated by Wassing et al., 2003, 2004. Attenuation studies have been initiated within the GEISER[4] project, allowing for a larger dataset on small and shallow induced earthquakes. Results are expected in 2012 and will be published.

Microearthquake investigations.
Early 2010 a new microseismic monitoring experiment was initiated at the location of the Bergermeer field, which is being developed as a gas storage facility. Monitoring was carried out for a period of 5 weeks, in which only the last three weeks gas was injected. A total of nine events were recorded after injection started and all were located near the central fault, which was thought to be the fault reactivated in the past with 4 events during the gas production phase (Kwee, 2011). After this period a continuous microseismic monitoring system was set-up and is operational since august 2010. Data are transferred in real-time to the KNMI and analysed. Results are incorporated in monthly reports issued by Taqa, the mining company that operates the gas-storage facility[5]. A traffic-light system[6] was designed in order to act in case of either an increase of microevents at a specific location or a larger event.

Systematic parameter correlation study.
A systematic parameter correlation study was published (Van Eijs et al., 2006). An update of this study is planned.

New developments
The build-up of the accelerometer network in the Groningen field enabled the use of waveform modelling at small epicentre distances using detailed local velocity models. Kraaijpoel and Dost, (2012) show that the local salt layer on top of the reservoirs in the most active north-western part of the Groningen field produces mode conversions that show as precursors to the direct S-phase. These precursors may help to constrain the depth of the source. In general, waveform modelling is expected to provide more insight in source location and attribution to existing faults.

In the seismic hazard calculations for the Netherlands, the EQRISK software has been used, based on the methodology of Cornell (1968) and McGuire (1976). Recently, a new methodology based on Monte Carlo inversion was tested for application to the hazard of natural seismicity in the south of the Netherlands (De Vos, 2010) and will be used in the next update of the hazard calculation for induced seismicity.

[4] Geothermal Engineering Integrating Mitigation of Induced Seismicity in Reservoirs-EU fp7 project http://www.geiser-fp7.eu/default.aspx
[5] http://www.gasopslagbergermeer.nl/downloads
[6] http://www.gasopslagbergermeer.nl/nieuws/TAQA_maatregelen_bodembeweging

7. Conclusions

The present update of the analysis of seismic hazard parameters for hydrocarbon exploitation, based on a seismicity database that nearly doubled in size since 2003, showed results consistent with the previous study (Van Eck et al., 2004). In addition, details on the development of seismicity, the difference in characteristics between the Groningen field and smaller gas fields and for the first time the mechanism of events in the Groningen field could be determined, which improves our understanding of the processes in the subsurface. However, uncertainties in the seismic hazard analysis are still large. The implications of the breakdown of stationarity, as was detected in the cumulative seismic energy release, should be considered in the next update of the seismic hazard analysis.

Attenuation relations for small-magnitude events, essential for hazard analysis, have been developed since 2003 (e.g. Bommer et al., 2007) and continue to be developed within GEISER. Accelerometer data are essential input for these studies. New hazard maps will be constructed after attenuation relations have been updated and Monte Carlo methods further adapted.

In a recent report on damage to buildings in Loppersum (De Lange et al., 2011), a community in the central part of the Groningen field, it is recommended to regularly update the M_{max} estimate and to install additional accelerometers in the region. The former is realized in the present publication, while the latter recommendation is being discussed with the NAM. Furthermore, initiatives are being prepared to increase the resolution of event location by detailed monitoring in specific areas.

Acknowledgements

We like to thank Chris Jansen for his continued technical assistance, Ko van Gend and Chris Meester for their efforts in the analysis of induced earthquakes and all those who contributed to discussions, TPA (Technical Platform on Earthquakes) and Tcbb (Technical Committee on Soil Movement) members.

References:

Anderson, J.G. and S. Hough, 1984, A model for the shape of the Fourier amplitude spectrum of acceleration at high frequencies, *Bull. Seism. Soc. Am., 74: 1969-1994*.

Atkinson, G.M., 1996, The High-Frequency Shape of the Source Spectrum for Earthquakes in Eastern and Western Canada, *Bull. Seism. Soc. Am*., 86:106-112.

Bender, B., 1983, Maximum likelihood estimation of b-values for magnitude grouped data, *Bull. Seism. Soc. Am., 73*: 831-851.

Begeleidingscommissie Onderzoek Aardbevingen (BOA), 1993. Eindrapport multidisciplinair onderzoek naar de relatie tussen gaswinning en aardbevingen in Noord-Nederland. 76pp.

Bommer, J., P.J. Stafford, J.E. Alarcon and S. Akkar, 2007, The influence of Magnitude Range on Empirical Ground-Motion Prediction, *Bull. Seism. Soc. Am.*, 97: 2152-2170.

Brune, J.N., 1970, Tectonic stress and the spectra of seismic shear waves from earthquakes, *Journal of Geophysical Research* 75, 26, 4997-5009.

Cornell, C.A., 1968, Engineering seismic risk analysis. *Bull. Seism. Soc. Am*., 58: 1503-1606.

Cosentino, P., V. Ficcara and D. Luzio, 1977, Truncated exponential frequency-magnitude relationship in earthquake statistics, *Bull. Seism. Soc. Am*., 67: 1615-1623.

De Crook, Th., B. Dost and H.W.Haak, 1995, Analyse van het seismische risico in Noord Nederland, *KNMI –Technisch rapport; TR-168*, 30pp.

De Crook, Th. And B.B.T. Wassing, 1996, Opslingering van trillingen bij aardbevingen in Noord-Nederland (*KNMI interim report*)

De Crook, Th., H.W. Haak and B. Dost, 1998. Seismisch risico in Noord-Nederland, *KNMI-Technisch rapport; TR-205*, 23pp.

De Lange, G., N.G.C. van Oostrum, S. Dorland, H. Borsje and S.A.J. de Richemont, 2011, Gebouwschade Loppersum, *Deltares report 1202097-000BGS-0003*, 84pp.

De Vos, D., 2010, Probabilistic Seismic Hazard Assessment for the Southern part of the Netherlands, *MSc Thesis, Utrecht University*, 58pp.

Dost, B. and H.W. Haak, 2002, A comprehensive description of the KNMI seismological instrumentation, *KNMI Technical report; TR-245*, 60pp.

Dost, B. and H.W. Haak, 2007, Natural and induced seismicity, in Th. E. Wong, D.A.J. Batjes, and J. de Jager, eds., *Geology of the Netherlands*, Royal Netherlands Academy of Arts and Sciences, 223-229.

Fernandez, A., R.R. Castro and C.I.Huerta, 2010, Spectral Decay Parameter Kappa in Northeastern Sonora, Mexico, *Bull. Seism. Soc. Am*., 100: 196-206.

Grob, M. And M. Van der Baan, 2011, Inferring in-situ stress changes by statistical analysis of microseismic event characteristics, The leading Edge, 30: 1296-1302.

Haak, H.W., B. Dost and F.H. Goutbeek, 2001, Seismische analyse van de aardbevingen bij Alkmaar op 9 en 10 september en Bergen aan Zee op 10 oktober 2001., *KNMI report TR-239*, 24pp.

Hager, B.H. and M.N. Toksoz, 2009, Technical review of Bergermeer seismicity study TNO report 2008-U-R1071/B, 6 November 2008, 34pp.

Hanka, W., J. Saul, B. Weber, J. Becker, P. Harjadi, Fauzi, and GITEWS Seismology Group: Real-time earthquake monitoring for tsunami warning in the Indian Ocean and beyond, Nat. Hazards Earth Syst. Sci., 10, 2611-2622, doi:10.5194/nhess-10-2611-2010, 2010.

Hanks, T.C. and H. Kanamori, 1979, A Moment Magnitude Scale, *Journal of Geophys. Research*, 84: 2348-2350.

Kraaijpoel, D. and B. Dost, 2012, Implications of salt-related propagation and mode conversion effects on the analysis of induced seismicity, *Journal of Seismology*, DOI: 10.1007/s10950-012-9309-4Online First™

Kwee, Jasper, 2011, Micro-seismicity in the Bergermeer gas storage field, *MSc thesis*, Utrecht University, 58pp.
(http://www.knmi.nl/research/seismology/PilotStudyBergermeer.pdf)

Logan, J.M., N.G. Higgs, J.W. Rudnicki, 1997, Seismicity risk assessment of a possible gas storage project in the Bergermeer field, Bergen concession, *Report to BP*, 137pp.

Marzocchi, W. and L. Sandri, 2003. A review and new insights on the estimation of the b-value and its uncertainty, *Annals of Geophysics*, 46: 1271-1282.

McGuire, R.K., 1976. FORTRAN computer program for seismic risk analysis. *Open-File report 76-67. US. Dep. Int., Geological Survey*, 90pp.

Muntendam-Bos, A.G., B.B.T. Wassing, C.R. Geel, M. Louh and K van Thienen-Visser, 2008, Bergermeer Seismicity Study, *TNO report 2008-U-R1071/B*, 95pp.

Page, R., 1968. Aftershocks and microaftershocks of the great Alaska earthquake of 1964, *Bull. Seism. Soc. Am.*, 58:1131-1168.

Roos, W., P.H. Waarts and B.B.T. Wassing, Kalibratiestudie schade door aardbevingen, *TNO-rapport: TNO-034-DTM-2009-04435*.

Rovelli, A., M. Cocco, R. Console, B. Alessandrini and S. Mazza, 1991, Ground motion waveforms and source spectral scaling from close-distance accelerograms in a compressional regime area (Friuli, northeastern Italy), *Bull. Seism. Soc. Am*., 81:57-80.

Schorlemmer, D., S. Wiemer and M. Wyss, 2005, Variations in earthquake-size distribution across different stress regimes, *Nature, 437*, no. 7058, 539-542.

Van Eck, T., 1988, Attenuation of Coda Waves in the Dead Sea Region, Bull. Seism. Soc. Am., 78: 770-779.

Van Eck, T. F. H. Goutbeek, H. Haak and B. Dost, 2004. Seismic hazard due to small shallow induced earthquakes, *KNMI-Scientific report; WR-2004-01*, 52pp.

Van Eck, T. F. H. Goutbeek, H. Haak and B. Dost, 2006, Seismic hazard due to small-magnitude, shallow-source, induced earthquakes in the Netherlands. *Engineering Geology*, 87: 105 -121.

Van Eck, T., F.H. Goutbeek and B. Dost, 2007, Site specific hazard estimates for the NUON energy plant in the Eemshaven, *KNMI intern report*, IR 2007-02, 17pp.

Van Eck, T., F.H. Goutbeek and B. Dost, 2008, Site specific hazard estimates for the LNG energy plant in the Europort area, *KNMI Internal Report* IR 2008-01, 16pp.

Van Eijs, R.M.H.E, F.M.M. Mulders, M. Nepveu, C.J. Kenter, B.C. Scheffers, 2006, Correlation between hydrocarbon reservoir properties and induced seismicity in the Netherlands, *Engineering Geology 84* (2006), p. 99–111.

Van Staalduinen, P.C. and C.P.W. Geurts, 1998, De relatie tussen schade aan gebouwen en lichte, ondiepe aardbevingen in Nederland: inventarisatie, *TNO-rapport: 97-CON-R1523-1*.

Wassing, B. B. T., 1998, Seismisch onderzoek te Zuidlaarderveen, *TNO-report NITG-98-141-B*

Wassing, B.B.T., D. Maljers, R.S. Westerhoff, J.H.A. Bosch, H.J.T. Weerts, 2003. Seismisch hazard van geïnduceerde aardbevingen. Rapportage fase 1. *TNO-rapport NITG 03-185-C.*

Wassing, B.B.T., D. Maljers, R.S. Westerhoff, J.H.A. Bosch, H.J.T. Weerts, A. Koopman, A. Dullemond, W. Roos, 2004. Seismisch hazard van geïnduceerde aardbevingen. Rapportage fase 2. *TNO rapport NITG 03-186-C*.

Weichert, D.H., 1980, Estimation of the earthquake recurrence parameters for unequal observation periods for different magnitudes, *Bull. Seism. Soc. Am., 70*: 1337-1346.

Appendix A: Midlaren, February 22-march 22, 2009

After a few small events detected at the end of February 2009 and located south-west of the Groningen field, a swarm of small events started March 12 of the same year and this activity continued for a period of 10 days. A total of 41 events were recorded, magnitudes vary from 0.2 to 1.4. Only 5 of these events did have a magnitude larger than 1.0. Due to the small size of the events, most were recorded in only 3 borehole stations. However, recordings of individual events show a high correlation (figure A1), enabling a relative location.

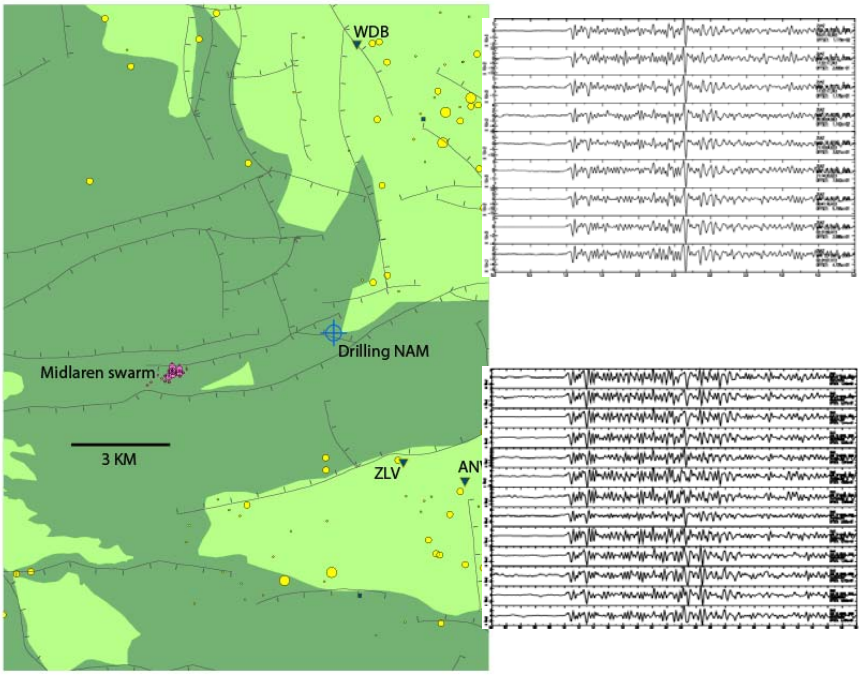

Figure A1. Epicenter map of the Midlaren events (purple circles), indicating the borehole stations that recorded the events (WDB, ZLV, ANV). Gas fields are indicated by light green, other induced events by yellow circles. Location of the NAM drilling is indicated in blue. Two panels (right) show the vertical component of station ZLV for two clusters of events.

Communication with NAM showed that there may have been a connection with a drilling activity (figure A1) at 4-5 km from the events at the same time, although the distance is quite large for a direct influence.

Appendix B. Fact sheet earthquake near De Hoeve, Friesland, at 26-11-2009

Introduction

In this report a first analysis was made of the earthquake in the southeast of the province of Friesland, near the Weststellingwerf- and Noordwolde gas fields. This earthquake has special importance, since there is no current gas extraction in the Weststellingwerf gas field, but instead water injection. The Noordwolde field is still in production. Vermillion is the current operator.

Instrumental parameters

The KNMI borehole network recorded the November 26 earthquake. Analysis resulted in the following parameters:

Origin time: 12h 54m 14.21 s
Epicenter: 52.892 N; 6.112 E
Dutch (Amersfoort) coordinates: X: 203.722 Y: 545.055
Magnitude (M_L): 2.8
Depth: 3 km

The error in the location coordinates is indicated in the figure below. The depth of the event is shallow, but hard to resolve with the current network. Therefore it is fixed at 3 km in the location procedure. Fixing the depth at 2 km results in a location 225m to the east and 114m to the north.

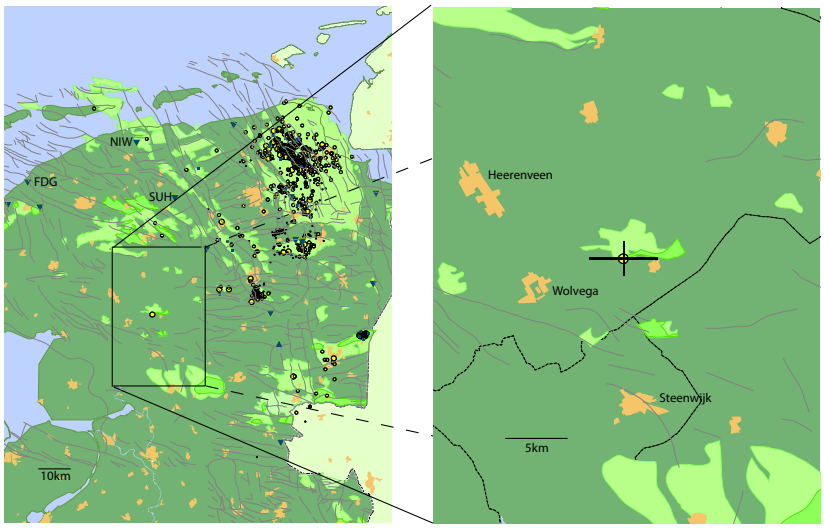

Figure B.1. Overview of induced seismicity (yellow circles) in northern Netherlands (left panel) and zoomed-in on the current event (right panel). The estimated error bars in the "De Hoeve" event are indicated.The Weststellingwerf gas field is situated directly north of the earthquake location. The Noordwolde gasfield is located at the south-eastern border of the Weststellingwerf gas field

Source mechanism:

Although the earthquake was recorded outside the KNMI borehole network, 3 more borehole sites were operating in an experimental setting at the time of the event. Two of them, Niawier (NIW) and Surhuizum (SUH), in the Northeastern part of Friesland and one north of Harlingen (Firdgum, FDG).

These new boreholes are very well located to provide additional information on the source mechanism, but are lacking a calibration of the sensors (polarity). This is planned. A first polarity check was done by looking at teleseismic events that produce enough high frequencies (> 1 Hz) to be detected in the borehole sensors. From this

first analysis the polarity of the vertical component could be determined. A first mechanism based on polarity data for the vertical component was determined.

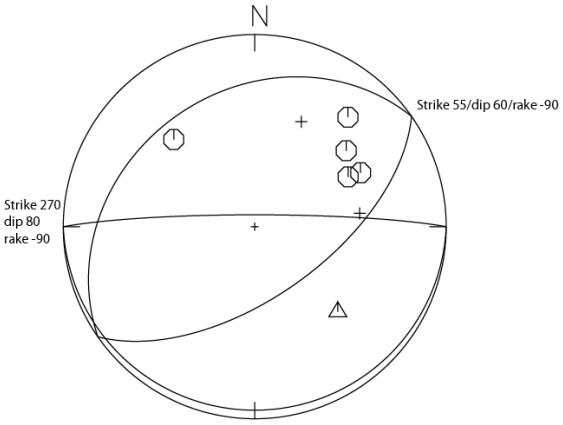

Figure B.2. Source mechanism retrieved from measured Z-polarities measured in the KNMI borehole network. Circles denote positive polarities, triangles negative polarities.

This means that the event could have two main solutions: 1] a steeply dipping (70-90 degrees) normal fault at a strike of 250-290 degrees, rake -90 degrees or 2] a reverse fault at a strike of 40-80 degrees and a dip between 60 and 70 degrees. Known faults in the region (Total, winningsplan Weststellingwerf and Noordwolde) are compatible with solution 1, which is therefore regarded as the preferred solution.

Source spectra

In addition to the mechanism, the spectra of the recordings provide information on other source parameters: seismic moment and derived moment magnitude, source radius, stress-drop and average displacement at depth. These parameters can be determined from spectra that are corrected for the instrument response and absorption/scattering. These corrections, a frequency dependent parameter kappa and a frequency independent Q_o, have been derived for each borehole station. The average value for kappa is 0.04s, the average value for Q is 50.

After correction, the following results have been obtained, assuming a circular Brune model:

Seismic moment: $M_0=1.3 \pm 0.9 * 10^{13}$ Nm with corresponding Mw=2.6±0.2
Source radius: r= 203 ± 25 m
Stress-drop: 8±7 bar
Displacement: 9± 7 mm

There are no reports of people that felt the earthquake in the epicentral area. This may be due to limited population in the area, since earthquakes from a magnitude 2.0 and up are usually reported to have been felt.

Appendix C. TNO-KNMI report on maximum damage due to induced earthquakes

TNO-KNMI rapport

Maximale schade door geïnduceerde aardbevingen: inventarisatie van studies met toepassingen op Bergermeer

Datum: 3 mei 2011

Auteurs:

Ir. W. van Kanten-Roos (TNO)
Dr. B. Dost (KNMI)
Prof. Ir. A.C.W.M. Vrouwenvelder (TNO)
Dr. T. van Eck (KNMI)

Samenvatting

Uit onderzoek van het KNMI en TNO naar de schade die op kan treden bij een ondiepe geïnduceerde aardbeving, blijkt dat schade alleen op hoofdlijnen is te kwantificeren. De kans op het ontstaan van (lichte) schade kan gekwantificeerd worden, er wordt echter in geen van de (in het verleden uitgevoerde) onderzoeken een uitspraak gedaan over de ernst van de schade bij grotere magnitudes. Hoewel er wel voortgang is geboekt met de schatting van de buitengrens van schade, is de verdere ontwikkeling van deze modellen afhankelijk van de beschikbaarheid van data voor schade veroorzakende aardbevingen. Deze dataset is klein en zal naar verwachting maar langzaam groeien. Ondanks dat de modellen niet gekalibreerd kunnen worden aan historische data en een betere gekwantificeerde voorspelling van het aantal woningen met schade op dit moment niet mogelijk is, is het wel mogelijk om een globale schatting te geven van de te verwachten ernst van de schade. Bestaande rekenmodellen laten zien hoe groot de kans is op lichte schade. De opgetreden schade bij een beving met magnitude M=3.5 laat zien dat ook matige schade kan ontstaan. Bij een aardbeving met magnitude M=3.9, de maximaal te verwachten beving, wordt verwacht dat het aantal schadegevallen met matige schade zal toenemen, maar niet dat er schade in een hogere categorie (aanzienlijke tot zware schade) zal ontstaan.

Inleiding

In Nederland gelden geen bouwvoorschriften voor belasting van trillingen buiten een gebouw. Er zijn wel richtlijnen beschikbaar, in de vorm van grenswaarden voor trillingssnelheden, waarbij bij overschrijding een (kleine) kans op schade bestaat (Stichting Bouw Research, SBR). De SBR richtlijn geeft overigens alleen aan dat bij overschrijding er schade kan ontstaan, het geeft geen informatie over de soort en ernst van de mogelijke schade. Trillingen als gevolg van geïnduceerde aardbevingen hebben een specifiek karakter, dat verschilt van natuurlijke aardbevingen. Het verschil zit vooral in de korte duur van de trilling in combinatie met een hoge maximale versnelling of snelheid van de grondbeweging. De oorzaak hiervan is dat geïnduceerde aardbevingen veel dichter bij het aardoppervlak plaats vinden dan tektonische (natuurlijke) aardbevingen. De kennis over geïnduceerde aardbevingen in Nederland is gebaseerd op observaties van de laatste 25 jaar (1986-2011). In deze periode is geen aardbeving geregistreerd van een sterkte (magnitude) groter dan M=3.5.

In dit rapport wordt een overzicht gegeven van de stand van zaken van onderzoek naar de relatie tussen de sterkte van geïnduceerde aardbevingen en de te verwachten schade. Vooral in de periode 2003-2004 is hier vooruitgang geboekt en dit heeft geresulteerd in een overzicht van de resultaten van deelstudies [7]

Relatie tussen trillingen en schade

Een uitgebreide studie van de relatie tussen de kans op schade aan gebouwen en geïnduceerde aardbevingen is in 1998 door TNO bouw uitgevoerd [2]. In deze studie is onderzoek gedaan naar het gebruik van de SBR richtlijn voor de inschatting van de kans op schade. Hierbij zijn versnellingsmetingen uit Noord-Nederland gebruikt. Resultaten van dit onderzoek zijn a] een inschatting van de kans op schade als functie van de maximale trillingssnelheid voor verschillende typen gebouwen (zie figuur 1) en b] een gemiddeld responsespectrum voor ondiepe aardbevingen in Noord-Nederland. Responsespectra geven inzicht in de mate waarin een gebouw reageert op een versnelling van de bodem. De vorm van het responsespectrum wijkt af van de Europese norm, zoals vastgesteld in Eurocode 8.

Wat kan er gebeuren

Gebaseerd op seismologische waarnemingen en kennis van de ondergrond zijn modellen gemaakt van wat er in de toekomst kan gebeuren, de zogenaamde hazardmodellen. Uitgaande van door het KNMI berekende hazard modellen [3][4] en door TNO berekende opslinger factoren als gevolg van de effecten van de ondiepe geologie [5][6], zijn kansmodellen voor het overschrijden van maximale versnellingen en daarvan afgeleide snelheden in Noord-Nederland ontwikkeld. De basis van deze hazardmodellen vormt de KNMI-database van geregistreerde aardbevingen in Noord-Nederland.

In [4] is de hazard berekend voor verschillende gasvelden, waaronder het Bergermeerveld. Schattingen van maximale snelheden van de bodembeweging voor dit veld zijn 40-60 mm/s voor een terugkeerperiode van de bevingen van T=10 jaar en T=100 jaar. Een terugkeerperiode van 10 jaar is ongeveer gelijk aan een 10% kans op het overschrijden van het maximum per jaar. Berekeningen zijn uitgevoerd voor een maximale magnitude van M=3.5. Aanpassing van deze waarde naar een M_{max} = 3.9 heeft een beperkt effect van ca 10-20% op deze waarden, aangezien de kans op optreden van grotere bevingen kleiner is, zodat de schatting van de maximale snelheden naar 50-70 mm/s gaat.

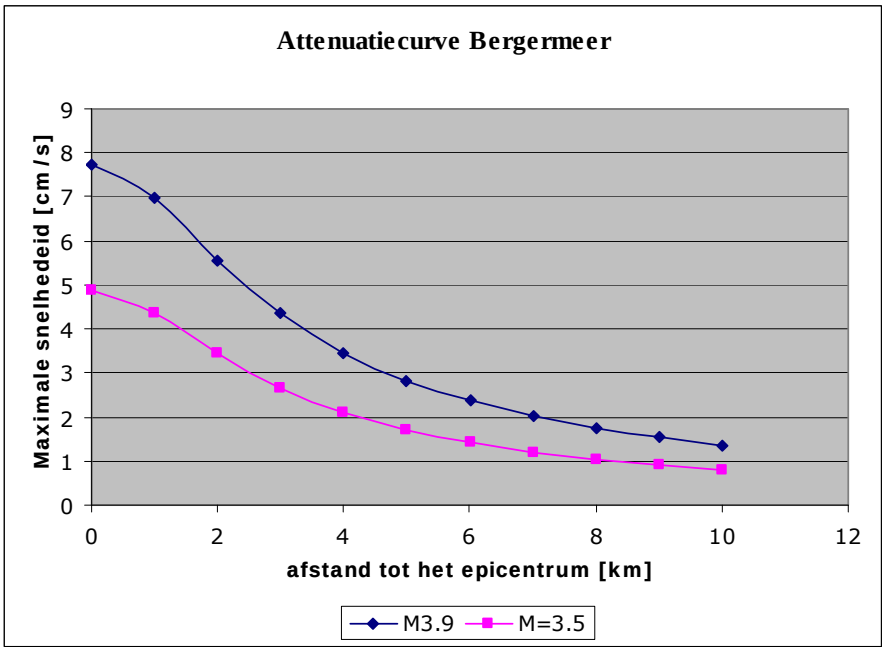

Figuur 1. Maximale snelheid van de grondbeweging als functie van de epicentrale afstand voor een bron op 2.2 km diepte.

Indien de bevingen van M= 3.5 en M=3.9 verondersteld worden met zekerheid op te treden in het Bergermeerveld ontstaan maximale snelheden (in het epicentrum) van 49 respectievelijk 77 mm/s. Dit volgt uit berekeningen op basis van empirische attenuatie functies, waarbij rekening gehouden is met de onzekerheid, door één keer de standaarddeviatie bij het resultaat op te tellen. De diepte van de aardbevingsbron is hierbij geschat op 2.2 km, de gemiddelde diepte van micro aardbevingen, die vanaf 2010 worden waargenomen in het Bergermeerveld met een set van trillingsopnemers (geofoons) op reservoir niveau.

Op een in dit geval altijd aanwezige afstand van epicentrum tot de rand van de bebouwing van 1 km is dit echter gedaald naar 43 en 69 mm/s. Uit figuur 2 is af te leiden dat deze maximale trillingssnelheden resulteren in ca 30 en 50% kans op schade voor een gebouw in goede staat. Op 3 km afstand zijn de maximale trillingssnelheden gedaald tot 27 en 44 mm/s (ca. 20 en 35% kans op schade).

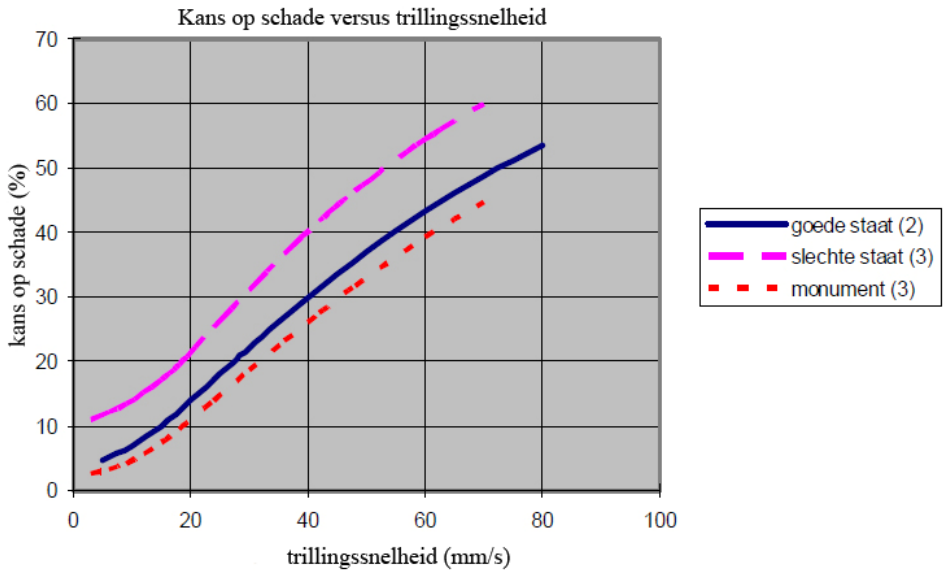

***Figuur** 2 Kans op schade als functie van de piekwaarde voor de trillingssnelheid, op de fundering gemeten, voor categorie 2 en categorie 3: onderscheid makend in monumenten en in slechte staat verkerende gebouwen (uit [9], naar [2]) Het woord "schade" houdt in: lichte, niet constructieve schade (zie tabel 1).*

Toetsing van modellen

In [5,6] is gekeken naar de validatie van hazardmodellen en de daaruit afgeleide schatting van de hoeveelheid woningen met schade. Voor Roswinkel bleek dat de verwachte aantallen woningen met schade veel hoger ligt dan het werkelijke aantal schademeldingen en dat de combinatie van de hazard kaarten en de SBR richtlijn (1% kans op schade) geen goed inzicht geeft in het totaal te verwachten aantal schadegevallen en de ernst van de schade [6, p26]. Aanbevolen werd een uitgebreidere kalibratie en validatie van de hazard en schade modellen uit te voeren. In 2007 is een vervolgrapport gemaakt [8], waarbij het doel was om tot een realistischer inschatting van de buitengrens van schade te komen, hetgeen vervolgens in [1] verder is uitgewerkt. De gevoeligheid van verschillende typen gebouwen is hierin onderzocht en er werd geconcludeerd dat de buitengrens voor schade beter bepaald kon worden. In de aanbevelingen wordt gemeld dat kalibratie met een groter aantal aardbevingen is aan te bevelen.

De huidige beschikbare dataset aan versnellingsmetingen is nog steeds beperkt en niet groot genoeg om een significante verbetering van de resultaten in bovengenoemde rapporten te bereiken. Vandaar dat het niet zinvol geacht wordt om op dit moment een nieuwe studie uit te voeren.

Schadebeoordeling

Het meest recente rapport over dit onderwerp [9] geeft niet alleen een uitleg over de materie, maar bevat ook een beschrijving van een gestandaardiseerde aanpak van het vastleggen en beoordelen van schade. Deze aanpak is vervolgens getoetst door toepassing op een vijftal geselecteerde panden in de provincie Groningen.

Beschouwing schade aan woningen in Bergen

De trillingssnelheden ter plaatse van de woningen zijn, uitgaande van het daadwerkelijk optreden van een M=3.9 aardbeving, zoals eerder afgeleid, maximaal 69 mm/s. Uit figuur 2 kan worden afgelezen dat bij een dergelijke trillingssnelheid de kans op schade voor de drie genoemde woningcategorieën als volgt is:

- Monumenten: 45%
- goede staat: 50%
- slechte staat: 60%

Op 3 km afstand is dit gereduceerd tot:

- Monumenten: 30%
- goede staat: 35%
- slechte staat: 45%

De ernst van de schade is hiermee nog niet gekwantificeerd. De ernst van schade kan primair worden onderverdeeld in (zie ook [9] en tabel 1):

- constructieve schade: veiligheid in het geding
- niet constructieve schade: veiligheid niet in het geding

Trillingen zullen bij lage snelheden geen constructieve schade tot gevolg hebben. Genoemde kansen zijn te relateren aan de kans van optreden van "niet constructieve schade". Niet constructieve schade [9] is weer onder te verdelen in schade met consequenties voor de esthetica, de gebruikswaarde en de levensduur. De EMS schaal definieert 5 gradaties van schade aan gebouwen welke is gekoppeld aan het type gebouw (klasse A tot en met F). Op basis van hun kwetsbaarheid voor schade worden gebouwen in 6 gebouwtypes ingedeeld:

A: los-gestapeld of klei
B: metselwerk en natuursteen
C: gewapend beton en degelijke houten constructies
D, E, F: gebouwen ontworpen met een zekere graad van aardbevingsbestendigheid.

De meeste bouwwerken in Nederland zijn opgetrokken uit metselwerk en kunnen geclassificeerd worden als type B. Dit zal ook voor de meeste woningen in Bergen gelden.

De gradaties zijn te beschrijven volgens de European Macroseismic Scale (EMS, [10]) als:

Gradatie (ref. EMS)	Klasse (type gebouw)	omschrijving
1		**Verwaarloosbare tot lichte schade (niet constructief)**
	A-C	haarscheurtjes in een enkele muur; neervallen van slechts kleine stukjes pleisterwerk; in een enkel geval vallen loszittende stenen van hogere delen van gebouwen.
	D-F:	kleine scheurtjes in pleisterwerk op regels en in scheidingswanden.
2		**Matige schade (licht constructief, matig niet-constructief)**
	A-C	scheuren in veel muren; vallen van grotere stukken pleisterwerk; delen van schoorstenen komen omlaag.
	D-F	haarscheurtjes in penanten, kolommen en balken; metselwerk valt uit voegen van wanden; scheuren in scheidingsmuren; vallen van stukken brosse afdeklagen en pleisterwerk.
3		**Aanzienlijke tot zware schade (matig constructief, zwaar niet-constructief)**
	A-C	in de meeste muren grote en diepe scheuren; dakpannen of leien glijden weg; schoorstenen breken op de daklijn; breuk van enkele niet-constructieve onderdelen.
	D-F	scheuren in penanten en losraken van stukken beton, scheuren in balken.
4		**Zeer zware schade (zwaar constructief, zeer zwaar niet-constructief)**
	A-C	ernstige breuken in muren; gedeeltelijk bezwijken van constructieve onderdelen
	D-F	ernstige schade door ontwrichting van het bouwskelet verwoesting van beton waarbij wapeningsstaal zichtbaar kan worden; gedeeltelijke instorting; penanten en kolommen komen scheef te staan
5		**Verwoesting (zeer zware constructieve schade)**
	A-F:	algehele of vrijwel totale ineenstorting.

Tabel 1. Classificatie van schade aan gebouwen (metselwerk), volgens [10].

De schade, die is ontstaan na de bevingen in 2001 met een magnitude van M=3.5 (lokale trillingssnelheid bij bebouwing 43 mm/s) en M=3.2, is in de meeste gevallen te karakteriseren als schade categorie 1, lichte schade en in een enkel geval schade categorie 2, matige schade (tabel 1).

Figuur 2 geeft aan wanneer lichte schade kan ontstaan. De figuur geeft echter geen informatie over de kans op *matige* schade. In [1] is geconcludeerd dat (een afgeleide van) de relatie uit figuur 1 voor het gebied rond Alkmaar conservatief is, dat wil zeggen: de relatie voorspelt meer schade dan in de praktijk is geclaimd. Indien deze theoretische inschatting desondanks wordt aangehouden dan zal de kans op matige schade bij een beving met magnitude M=3.5 liggen in de orde van 5%. Zwaardere schade is bij deze magnitude niet voorgekomen.

Wordt vervolgens uitgegaan van een gelijk verloop van de curve voor matige schade, dan volgt hieruit dat de (conservatieve) kans op matige schade bij een aardbeving met een magnitude van M=3.9 (lokale snelheid bij bebouwing 69 mm/s) als volgt is:

- monument: 20%
- goede staat: 25%
- slechte staat: 35%

Schade in categorie 3 (aanzienlijke tot zware schade) wordt niet verwacht. De ervaring leert, dat deze schade bij natuurlijke aardbevingen kan optreden bij snelheden boven de 100 mm/s.

Geconcludeerd wordt dat als een aardbeving met magnitude M=3.9 optreedt er in een aanzienlijk aantal gebouwen matige schade wordt verwacht maar nog geen schade uit de categorie 3. Concreet betekent dit dat er bij meer gebouwen scheuren in muren kunnen worden geconstateerd, dat er grotere stukken pleisterwerk kunnen vallen en in uitzonderingsgevallen delen van schoorstenen omlaag kunnen komen.

Opgemerkt wordt dat de uiteindelijke schade afhangt van het type en de staat van het gebouw ter plaatse. In dit rapport is niet naar individuele gevallen gekeken.

Referenties:

1. Roos, W., P.H.Waarts en B.B.T. Wassing, 2009, Kalibratiestudie schade door aardbevingen, *TNO rapport TNO-034-DTM-2009-04435*, 33pp.
2. Van Staalduinen, P.C. en C.P.W. Geurts, 1998, De relatie tussen schade aan gebouwen en lichte, ondiepe aardbevingen in Nederland: inventarisatie, *TNO rapport 97-CON-R1523-1*, 98pp.
3. Van Eck, T., F. Goutbeek, H. Haak & B. Dost, 2003, Seismic hazard due to small shallow induced earthquakes. *KNMI-publicatie: WR-2004-01*, ISBN 90-369-2248-8.
4. Van Eck, T., F.H. Goutbeek, H.W. Haak en B. Dost, Seismic hazard due to small-magnitude, shallow-source, induced earthquakes in the Netherlands, *Engineering Geology*, 2006, **87**, 105-121, doi:10.1016/j.enggeo.2006.06.005.
5. Wassing, B.B.T, D. Maljers, R.S. Westerhoff, J.H.A. Bosch en H.J.T. Weerts, 2003, Seismische hazard van geïnduceerde aardbevingen, rapportage fase 1, *TNO-rapport NITG 03-185-C*, 77pp
6. Wassing, B.B.T, D. Maljers, J.H.A. Bosch en H.J.T. Weerts, A. Koopman, A. Dullemond, W. Roos, 2004, Seismische hazard van geïnduceerde aardbevingen, rapportage fase 2, TNO-rapport NITG 03-186-C, 31pp
7. Wassing, B.B.T., T. van Eck en R.M.H.E. van Eijs, 2004, Seismische hazard van geïnduceerde aardbevingen: Integratie van deelstudies, TNO rapport NITG 04-244-B; KNMI-publicatie 208, 10pp.
8. Wassing, B.B.T., P.H.Waarts en W. Roos, 2007, Kalibratie van hazard- en schademodellen Seismisch risico geïnduceerde aardbevingen, TNO-rapport 2007-U-R0407/B, 34pp.

9. De Lange, G., N.G.C. van Oostrom, S. Dortland, H. Borsje en S.A.J. de Richemont, 2011, Gebouwschade Loppersum, Deltares report 1202097-000-BGS-0003, 84pp.
10. Grünthal, G., 1998, "European Macroseismic Scale 1998", Cahiers du Centre Europeen de Geodynamique et de Seismologie, Luxembourg 1998; Vol 15, 99pp.

A complete list of all KNMI-publications (1854 – present) can be found on our website

www.knmi.nl/knmi-library/knmipub_en.html

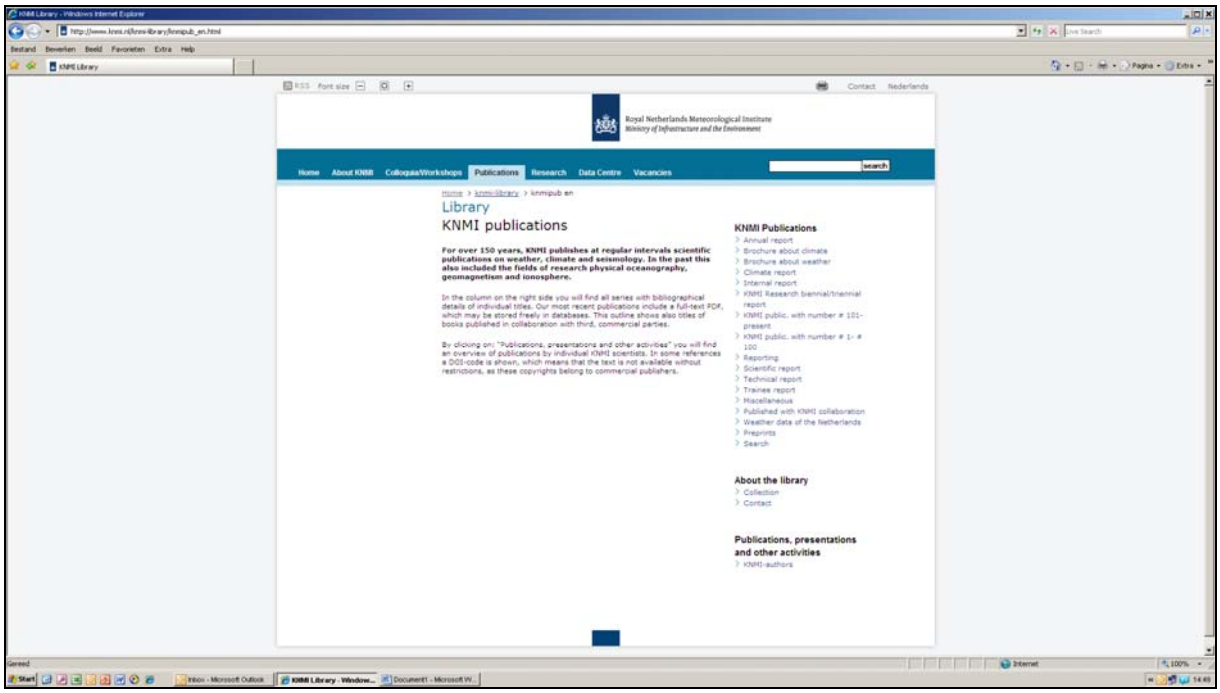

The most recent reports are available as a PDF on this site.